

Article

Quantum Chemical Approach to the Adsorption of Chlorpyrifos and Fenitrothion on the Carbon-Doped Boron Nitride Nanotube Decorated with Tetrapeptide

Chien-Lin Lee and Chia Ming Chang * 

Environmental Molecular and Electromagnetic Physics (EMEP) Laboratory, Department of Soil and Environmental Sciences, National Chung Hsing University, Taichung 40227, Taiwan

* Correspondence: abinitio@dragon.nchu.edu.tw

Abstract: In the present study, four materials based on boron nitride nanotubes—namely pristine BNNT, C-doped BNNT, tetrapeptide/BNNT, and tetrapeptide/C-doped BNNT—were examined to evaluate adsorption of the organophosphorus pesticides chlorpyrifos and fenitrothion. Through a quantum chemical approach to the molecular and electronic structures, the impacts of C doping and tetrapeptide modification on boron nitride nanotubes are clarified. The results reveal that the tetrapeptide decoration does have the potential for differential sensing of chlorpyrifos and fenitrothion, but the improvement in the adsorption characteristics is slightly inferior to that of the C doping method. Nanosensors, such as C-doped BNNT and tetrapeptide/C-doped BNNT, are used to monitor chlorpyrifos and fenitrothion in solution phase, respectively. This quantum chemistry investigation has paved the way for the design of differential sensing devices for organophosphorus pesticides.

Keywords: organophosphorus pesticide; boron nitride nanotube; tetrapeptide; carbon doping; quantum chemical method



Citation: Lee, C.-L.; Chang, C.M. Quantum Chemical Approach to the Adsorption of Chlorpyrifos and Fenitrothion on the Carbon-Doped Boron Nitride Nanotube Decorated with Tetrapeptide. *Crystals* **2022**, *12*, 1285. <https://doi.org/10.3390/cryst12091285>

Academic Editors: Jesús Sanmartín-Matalobos and Eamor M. Woo

Received: 16 August 2022

Accepted: 8 September 2022

Published: 11 September 2022

Publisher's Note: MDPI stays neutral with regard to jurisdictional claims in published maps and institutional affiliations.



Copyright: © 2022 by the authors. Licensee MDPI, Basel, Switzerland. This article is an open access article distributed under the terms and conditions of the Creative Commons Attribution (CC BY) license (<https://creativecommons.org/licenses/by/4.0/>).

1. Introduction

Organophosphorus (OP) pesticides have been widely utilized in agricultural activities. Because of their low solubility and low degradability, they readily remain in soil or groundwater. Previous literature revealed that there are higher health risks from OP pesticides in groundwater than in soil (at the regional scale), suggesting an urgent need for groundwater protection [1].

The conductivity is not as good when attempting to use boron nitride nanomaterials as the sensor matrix as it is when using carbon nanotubes or graphene, due to the wide bandgap of 5.5 eV [2]. In order to improve the performance of boron nitride nanotubes (BNNTs), several past studies suggest doping impurity atoms or transition metals to enhance their reactivity. For example, the Si-doped BNNT [3] and Fe-doped BNNT [4] improve electronic properties by altering electrostatic potential as well as HOMO and LUMO energy levels for adsorbing organophosphorus pesticides.

The geometry and electronic structure of C-doped boron nitride nanotubes have been investigated using hybrid Heyd–Scuseria–Ernzerhof density functional theory with HSE06/6-31G level, and the results reveal that the reduction of the first, second and third optical transitions is sensitive to the number of dopants [5]. The findings described above stem from the high spin density and charge density introduced by C doping [6]. Fermi energies, energy bands and density of states on zigzag- and armchair-carbon-doped BNNT were compared with those of pure BNNT. It was found that the bandgaps of both were reduced due to substitution of boron or nitrogen atoms with carbon atoms [7,8]. Further understanding of the chirality of nanotubes was based on a previous study, which showed that doped nanotube derivatives, especially armchair form nanotubes, make for stronger adsorption of organophosphates compared to pristine nanotubes [9]. C-doped BNNT not only

changes the internal electronic structure, but also increases the adsorption capacity when forming chemical bonds or non-covalent interactions with external molecules [10], which improves the redox reaction of the compound through stronger electron donor–acceptor transfer. Hirshfeld charge density analysis revealed that the electron-rich C-BNNS strongly activates the reduction of N_2O molecules through electron donation [11]. Furthermore, carbon doping and the defective structure contribute to promoting the performance of N_2 reduction reaction on C-BN catalyst, with excellent stability [12].

After absorption and digestion, OP pesticides have a significant inhibitory effect on acetylcholinesterase (AChE), and AChE-reactivating drugs do not benefit poisoned humans, which causes damage to biological health and food safety. The active site of *Torpedo californica* AChE (TcAChE) bound with DFP, sarin, and soman has been proved by X-ray crystallography [13]. Previous studies have simulated tetrapeptide His-Glu-Pro-Ser from the binding site of acetylcholinesterase; it was found to exhibit good binding constants with organophosphorus or carbamate pesticides (i.e., paraoxon, carbaryl) [14,15].

In recent years, biotic–abiotic interfaces have been explored and applied to the development of electronic devices such as sensors. The AChE electrochemical biosensor has been successfully used to measure low- and medium-concentration organophosphorus compounds in the liquid phase [16] and the gas phase [17]. In this type of sensor, the enzyme AChE has been immobilized on nanomaterials such as multi-walled carbon nanotubes, gold nanoparticles, or quantum dots, which has significantly contributed to the enhancement of OP pesticide determination [18]. From the results of DFT calculations, due to the polarity of BN nanosheets, the affinity for amino acids through weak physical adsorption is stronger than that of graphene [19]. In addition, when chlorpyrifos is used as a model compound, the biosensor shows a wide range, low detection limit, and good reproducibility [20]. Previous literature demonstrated that several problems, such as enzyme loss and response time, are solved with high stability [21]. In this way, the present study is inspired to design a BN-based biosensor with higher sensitivity and selectivity to OP pesticides [22].

The design of biosensors inevitably involves biochemistry and materials science, and weak intermolecular interactions such as van der Waals interactions, hydrogen bonds, and repulsive steric interactions have attracted interest in non-covalent interactions (NCIs) as an important factor for consideration. Some quantum chemical methods containing topological analysis of the Electron Localization Function (ELF) [23] and Quantum Theory of Atoms in Molecules (QTAIM) [24] were implemented to provide a deeper insight into the nature of interactions. These methods mentioned above are esoteric, but somewhat elegant, and they have formed the overarching approach, Quantum Chemical Topology (QCT), which has been successfully employed to describe and understand the chemical reactivity of molecules [25–27].

The conductivity of carbon-doped boron nitride nanotubes is between that of pure carbon and that of boron nitride nanotubes [28,29]. The tetrapeptide His-Glu-Pro-Ser, with a negatively charged carboxylate and a positively charged ammonium group, points to the aqueous solution, helps to dissolve in water [30], and binds pesticides with high affinity [31]. However, little study has been conducted on the combination mentioned above. Therefore, in addition to BNNT, C-doped boron nitride, and tetrapeptide/boron nitride, tetrapeptide/C-doped boron nitride is the fourth hypothetically ideal material used in this study. The objective of this study is to elucidate whether it can show synergistic effects through the strategy of C-doping and tetrapeptide decoration to improve the sensitivity of the detection for chlorpyrifos and fenitrothion. It is beneficial for developing boron-nitride-based metal-free biosensors with low cost and high sensitivity.

2. Computational Details

The armchair (5,5) boron nitride nanotubes, whose edges are terminated by mono-hydrogen with and without one hexagonal carbon island, are performed by Nanotube Modeler software (JCrystalSoft, 2018) to generate the XYZ coordinates of models. The

tetrapeptide His-Glu-Pro-Ser is in zwitterionic form. The protonation state of residues comes from the experimental evidence. Creating this tetrapeptide-decorated pristine BNNT and C-doped BNNT through the strategy of adsorption, the geometries and electronic structures are then calculated by MOPAC 2016, which is a semiempirical quantum chemistry software [32] and is available from <http://openmopac.net> (accessed on 15 July 2021). The molecular mechanics correction for the amidic bonds (CONH) is applied. In this study, the subsequent computational steps are used for organophosphorus pesticides, including chlorpyrifos (chl) and fenitrothion (fen), due to the high binding constant with tetrapeptide His-Glu-Pro-Ser (Mascini, 2008 #7). The geometric structure databases of organophosphorus pesticides listed above are downloaded from PubChem. The approaches for this study are implemented by the semiempirical PM7 method from *d*. The geometries of all systems are fully optimized using tight optimization criteria with a gradient threshold of $4.2 \times 10^{-4} \text{ kJ mol}^{-1} \text{ \AA}^{-1}$. The solvent effect is implicitly treated by the conductor-like screening model (COSMO), which uses a dielectric constant of 78.4 and an effective radius of 1.3 Å for water (Klamt, 1993 #6).

A view of electrostatic interaction and hydrogen bonding emerges as continuous surfaces to show non-covalent intermolecular and intramolecular interactions (NCI) [33,34]. Then, the graphical and numerical comparative results of equilibrium structures, Mulliken charges and electrostatic potential from PM7 level are illustrated by the MoCalc 2012 software. Fukui's FMO susceptibilities for predicting the most reactive position on chemical species perform molecular orbitals [35], the nucleophilicity, and electrophilicity, which are related to HOMO and LUMO, respectively, as shown by the Mayr equation [36].

3. Results and Discussion

3.1. Non-Covalent Interaction (NCI)

There are sporadic blue areas between the pyridine of chlorpyrifos and BN55-CC1. For polar molecules with intrinsic dipole moment and a lone pair, the additional term corresponding to the dipole–dipole interactions arises (Petruşhenko, 2017 #16). Thus, its non-covalent interaction distribution area is wider than that between the benzene structure of fenitrothion and BN55-CC1. Meanwhile, chlorine atoms bonded to the pyridine also have significant interactions. The adsorption site is primarily from the thiophosphate group, and contribution of van der Waals interaction is a critical factor in the adsorption of organophosphorus pesticides such as chlorpyrifos on the surface, as well as overlapping [4]. Although the phosphorothioate of fenitrothion has little repulsion, the oxygen atoms are a dark blue color, which indicates the main non-covalent interaction site that can be strongly adsorbed by BN55-CC1 (Figure 1).

After the tetrapeptide is added, many blue–green areas between tetrapeptide and chlorpyrifos are overlapping with the formation of hydrogen bonds, but there is a large red area in the C-doped site, where the carbon branch of Glu is just close enough that it is causing repulsion, and other color distributions are more dispersed after co-adsorption. See Figure 1D: the red area of fenitrothion on BN55-CC1 is decreased, and there are many blue areas dotted between the tetrapeptide and BN55-CC1, especially between the hydrogen bonded on nitrogen of Ser, oxygen on amide of Pro and the C-doped site. However, the overall distribution of non-covalent interactions is looser.

Due to the weaker aromaticity for N-heterocycles, experimental evidence indicates that the binding of protein/peptide to pristine carbon nanotubes in aqueous solutions is related to hydrophobic interaction (apart from the π - π stacking interaction) [37]. As for BNNTs, fluorescence and infrared absorption spectra suggest strong π - π interactions between the adsorbent and the peptide [38]. Different functional groups exhibit different mechanisms of reaction: π -systems presented on aromatic rings (e.g., phenyl, phenol, indole, and imidazole) are primarily favorable for adsorption energy, and secondary ones are single double bond (e.g., COOH, CONH₂, and CONHCH₃), whereas the NH₂ and OH adsorption originates from CH- π interactions [39].

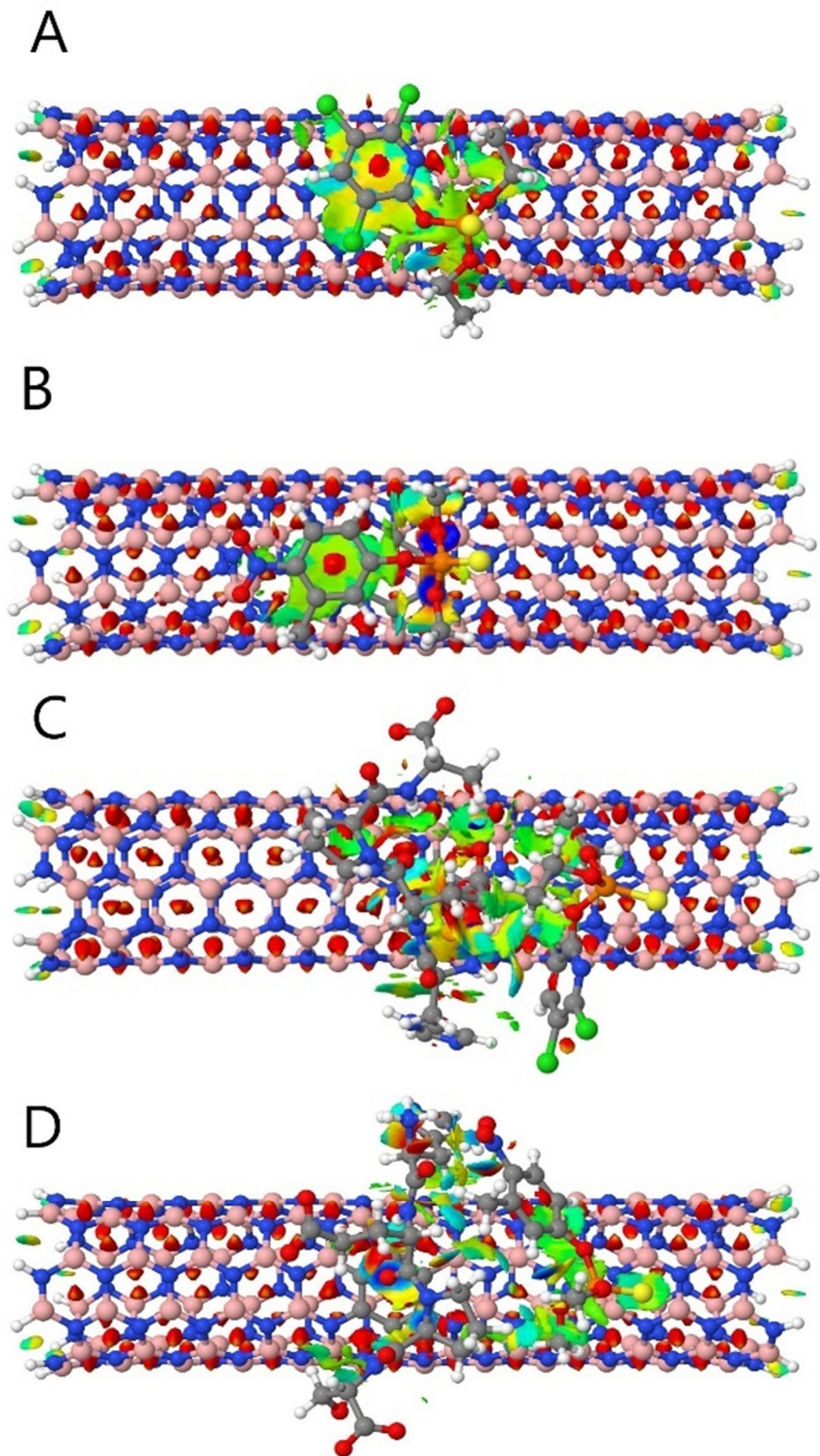


Figure 1. Non-covalent interaction between pesticides (chlorpyrifos (chl) and fenitrothion (fen)) and carbon-doped armchair (5,5) boron nitride nanotube (BN55-CC1) without (A,B) and decorated with tetrapeptide (4pep) (C,D).

3.2. Semiempirical PM7 Optimized Geometry and Reaction Enthalpy

Under co-adsorption conditions, as shown in Figure 2, the hydrogen bonds between chlorpyrifos and the tetrapeptide occur at the chlorine atom adjacent to the oxygen atom and at the hydrogen on the amide nitrogen of His (2.83 Å). In diagram (A), the tetrapeptide has more intramolecular hydrogen bonds: up to four (1.45 Å, 1.71 Å, 2.16 Å, and 3.05 Å). In particular, there are three bonds between Glu and Ser residues. This phenomenon makes the molecules closer through hydrogen bonds. As for fenitrothion, there is an intermolecular hydrogen bond between its nitro group and the hydrogen on the amide nitrogen of His, and the distance is shorter by 0.73 Å, but there is no intramolecular hydrogen bond. In fact, pesticide receptors such as paraoxon and carbaryl (with designed residues) are able to interact with the template predominantly through electrostatic, van der Waals interactions, and hydrogen bonds [15]. From BN55-CC1 modified by tetrapeptide, it has a hydrogen bond during co-adsorption with fenitrothion; the amino group of Ser actually forms a 2.58 Å hydrogen bond with the C-doped site on BN55-CC1, which plays a vital role.

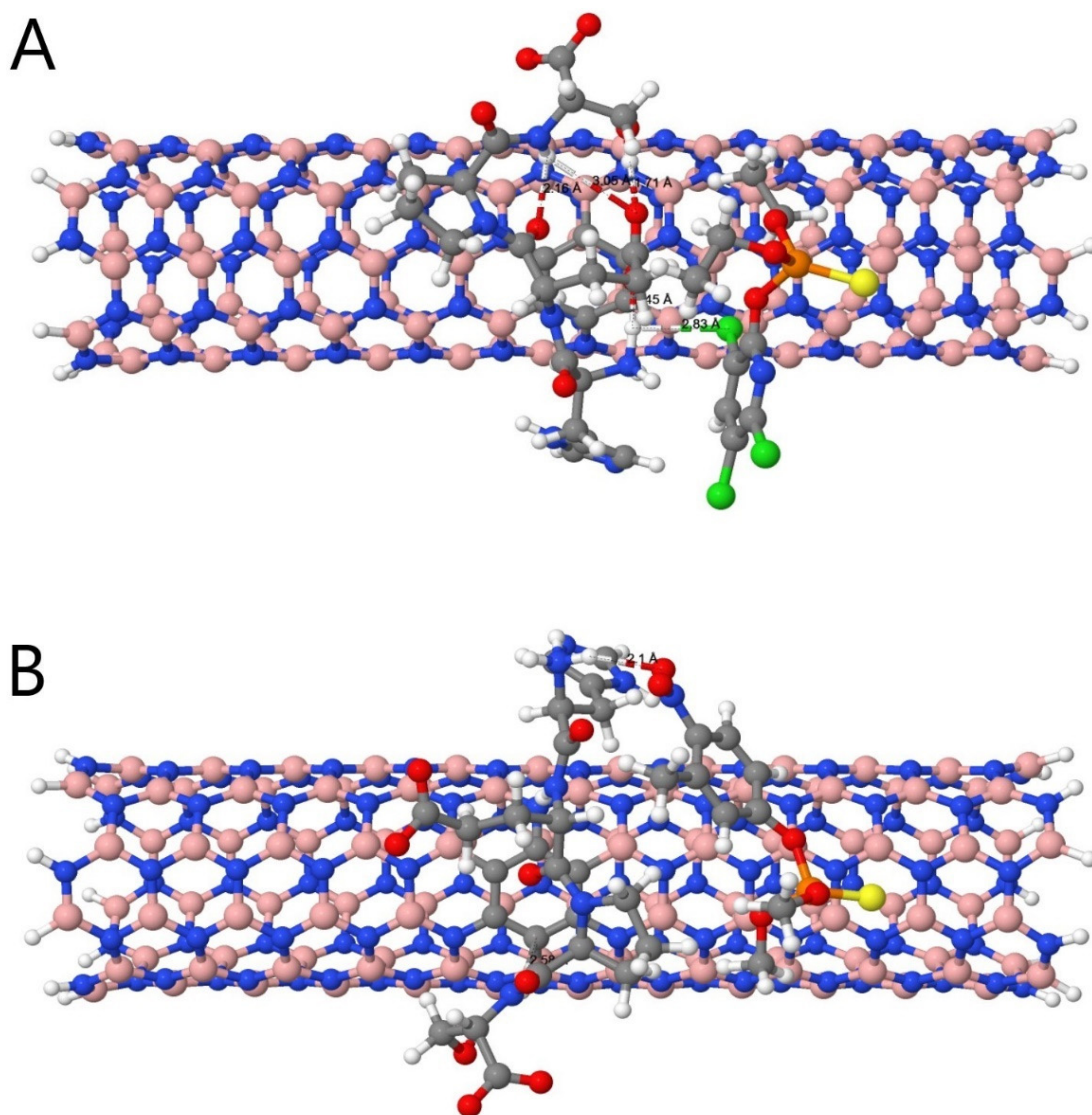


Figure 2. Equilibrium structures of pesticides ((A) chlorpyrifos (chl) and (B) fenitrothion (fen)) adsorbed on carbon-doped armchair (5,5) boron nitride nanotube (BN55-CC1) decorated with tetrapeptide (4pep).

It is well known that pollutants will have different physical and chemical properties under various environmental conditions. First, we analyzed the reaction enthalpy of gaseous and aqueous pollutants when they are adsorbed. It can be seen from Table 1 that regardless of whether BN55 is C-doped or not, more adsorption energy is released when pollutants combine with BNNT in an aqueous solution, indicating that removing both pollutants in an aquatic environment is helpful and the efficiency can be improved. Thus, in the next section, we consider the difference in electronic structure in gas phase and aqueous solution, with aqueous state as the important research objective. With pristine BNNT as the substrate, the adsorption performance of chlorpyrifos is better than that of fenitrothion. However, when the adsorbent is BN55-CC1, the adsorption energy of chlorpyrifos decreases due to the lessened polarity on the C-doped site, whereas that of fenitrothion increases, and even the degree of change in the adsorption result of the aqueous solution state is greater.

Table 1. Reaction enthalpy (ΔH_f in kcal/mol) of chlorpyrifos (chl) and fenitrothion (fen) adsorbed on carbon-doped armchair (5,5) boron nitride nanotube (BN55-CC1) without and decorated with tetrapeptide (4pep).

			Reaction Enthalpy (ΔH_f) (kcal/mol)
BN55	+chl	→BN55_chl	−39.0
BN55	+fen	→BN55_fen	−27.1
BN55_CC1	+chl	→BN55_CC1_chl	−38.2
BN55_CC1	+fen	→BN55_CC1_fen	−29.1
BN55_s	+chl_s	→BN55_chl_s	−46.6
BN55_s	+fen_s	→BN55_fen_s	−32.8
BN55_CC1_s	+chl_s	→BN55_CC1_chl_s	−41.9
BN55_CC1_s	+fen_s	→BN55_CC1_fen_s	−37.2
BN55_s	+4pep_s	→BN55_4pep_s	−44.7
BN55_CC1_s	+4pep_s	→BN55_CC1_4pep_s	−41.6
BN55_4pep_s	+chl_s	→BN55_4pep_chl_s	−20.9
BN55_4pep_s	+fen_s	→BN55_4pep_fen_s	−31.2
BN55_CC1_4pep_s	+chl_s	→BN55_CC1_4pep_chl_s	−4.5
BN55_CC1_4pep_s	+fen_s	→BN55_CC1_4pep_fen_s	−32.2

After BN55_s is decorated, the adsorption energy is indeed reduced with the addition of pollutants, except for fenitrothion adsorbed by BN55-CC1_s. For the data summarized in Table 1, the adsorption enthalpy produced by BN55-CC1 and BN55-4pep adsorbing pollutants in water shows that the former is has greater potential as a material. In addition, it is undeniable that the energy released from chlorpyrifos and fenitrothion during adsorption is the inverse when the adsorbent is BN55-4pep_s, which is related to the stronger affinity between the tetrapeptides and fenitrothion. A strong interaction forms covalent binding between the pesticide dichlorvos and the serine residue from the hexapeptide ($\text{NH}_3^+\text{-Glu-His-Gly-Gly-Pro-Ser-COO}^-$) [40]. However, from the analysis of the change in reaction enthalpy, such a covalent bond does not seem to exist. When applying BN55-CC1-4pep_s, the adsorption effect of fenitrothion is far better than that of chlorpyrifos. For fenitrothion, whether the tetrapeptide is involved in co-adsorption or not, C-doping promotes improved adsorption capacity.

From a general point of view, all adsorptions appear as exothermic reactions. BN55_s is selected as the most stable system to immobilize chlorpyrifos, and BN55-CC1-4pep_s produces the most unstable structure when adsorbing chlorpyrifos. For adsorbing feni-

trothion, BN55-CC1_s is the primary adsorbent, and the secondary adsorbent is BN55_s or BN55-CC1-4pep_s.

3.3. Electrostatic Potential

Before decoration of tetrapeptide the surface charge of BN55-CC1 shows no difference in Figure 3A,B. The negative charge of chlorpyrifos is mainly concentrated in the phosphorothioate region and in the vicinity of the nitrogen atom of pyridine. There are many negative charges in the nitro group, including phosphorothioate for fenitrothion. These polar positions are active sites for reaction; that is, electrons are concentrated, consistent with the main force of adsorption. The co-adsorption of the tetrapeptide alters the distribution position of charges. The negative charges are condensed in the carboxylic acid of Ser (Figure 3C) and carboxylic acids of Ser and Glu (Figure 3D). The positive charges are mainly concentrated in the pyridine of His instead of the pollutants themselves, indicating the area around the functional group of the tetrapeptide is where electrons mainly flow out. Charged groups reflect the amphiphilic tetrapeptide dissolving in water easily, which may protect functionalized-surface boron nitride nanotubes from aggregation as well because of electrostatic repulsion and dispersion [41]. Except for the edges of the boron nitride nanotubes, the state of charge on the surface of BN55-CC1-4pep and BN55-CC1-adsorbing chlorpyrifos far exceeds that of the nanotubes when the adsorbate is fenitrothion, and all charges are almost positive. The colors on BN55-CC1-4pep all are blue, suggesting that the probability of charge transfer and the stability of the electronic structure are reduced.

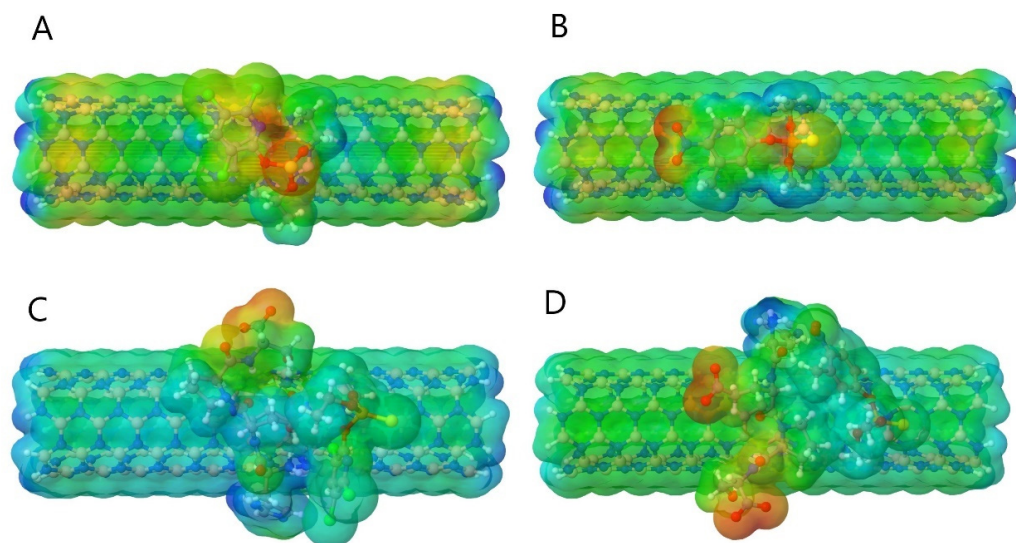


Figure 3. Electrostatic potential of pesticides (chlorpyrifos (chl) and fenitrothion (fen)) adsorbed on carbon-doped armchair (5,5) boron nitride nanotube (BN55-CC1) without (A,B) and decorated with tetrapeptide (4pep) (C,D).

3.4. Frontier Molecular Orbital Electrophilic Susceptibility

As shown in Figure 4, no matter what the adsorbate is, C-doped sites in BN55-CC1 are more susceptible to electrophilic attack, the active site is shown as an electron donor, and the nitrogen atom has a property of high electronegativity, making the blue in the reaction zone darker. A similar electrophilic reaction is verified by [42]. BN55-CC1-4pep exhibits unsatisfactory electrophilic susceptibility when interacting with chlorpyrifos. The red color becomes obvious, and the electron flow rate of BN55-CC1-4pep is blocked therein. On the contrary, when the tetrapeptide and fenitrothion are co-adsorbed, the distribution points of electrophilic susceptibility increase, which means it has nucleophilic characteristics. As a result, the decoration contributes to the reactivity of the electron donor due to the tetrapeptide for fenitrothion.

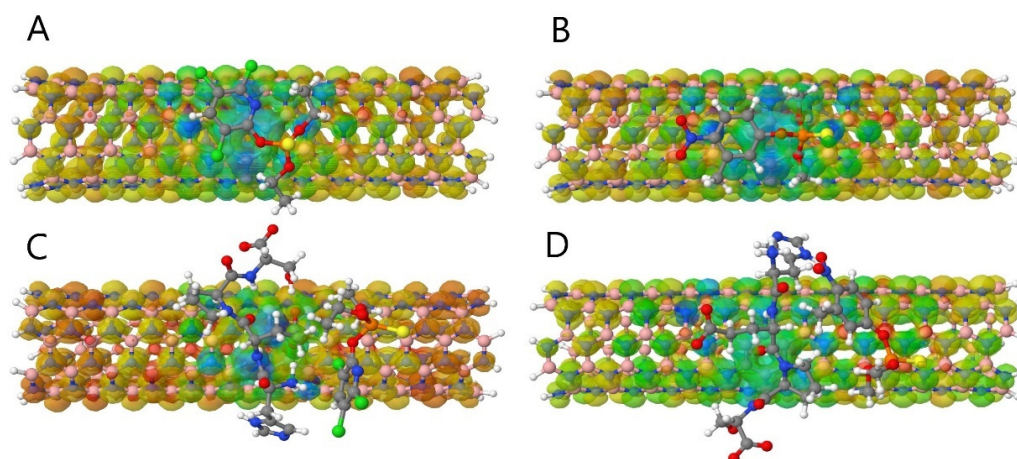


Figure 4. Frontier molecular orbital electrophilic susceptibility of pesticides (chlorpyrifos (chl) and fenitrothion (fen)) adsorbed on carbon-doped armchair (5,5) boron nitride nanotube (BN55-CC1) without (A,B) and decorated with tetrapeptide (4pep) (C,D).

3.5. Hard and Soft Acid and Base (HSAB)

The ionization energy is described by the negative of the HOMO, and the electronic affinity by the negative of the LUMO energy. The two substrates, including BN55 and BN55-CC1, change the electronic structure through the environment. The decrease in ionization energy, electron affinity, and electronegativity values clearly indicates that the attraction of electrons is weakened, changing from a gaseous state to an aqueous state (Table 2). The descriptors of chlorpyrifos and fenitrothion show the opposite performance. When the electronegativity difference between the adsorbent and the compound increases, a stronger interaction is generated, so the adsorption enthalpy increases in solution.

The ionization energy of BN55 is greater than that of BN55-CC1, and the electron affinity shows $\text{BN55-CC1} > \text{BN55}$, but the difference is only within the range of 0.1 eV, so the impact is minimal. The electronegativity of the carbon atom is between that of the boron atom and the nitrogen atom. After C-doping, the partial charge is not as good as for the original boron nitride nanotube, so the electronegativity is slightly smaller. The values of ionization energy, electron affinity, and electronegativity for BN55 also effectively reduce after adsorbing tetrapeptide. However, compared with the above-mentioned materials, BN55-CC1-4pep causes the greatest degree of change. Even though chlorpyrifos has more chlorine atoms, it is not in the same orbital with other atoms, and electrons are difficult to transfer among the molecule. In addition, fenitrothion has a larger conjugated system, which is beneficial to the stability of electrons; hence the ionization energy, electron affinity, and electronegativity are greater than that of chlorpyrifos.

Chemical potential ($\mu = -(I + A)/2$) is the negative value of electronegativity. According to the electronegativity data in the table, the pristine boron nitride nanotubes are still highly attractive to electrons at this time, so the electrons flowing to pollutants is not a perfect result. Not only the aqueous solution but also the addition of tetrapeptide and C-doping can promote an increase in chemical potential, especially for BN55-CC1-4pep, which displayed the highest chemical potential. While the two pollutants are dissolved in water the chemical potential energy is reduced, and this can also prove the conclusion that BN55-CC1 and BN55-CC1-4pep are electron donors, resulting in the enhancement of electron transfer.

The electrophilic index ($\omega = \mu^2/2\eta$) of pollutants in aqueous solution has become larger, which is consistent with the electronegativity results. Except for BN55-CC1 and compared with BN55, the index value is much smaller after decoration of tetrapeptide. These changes emphasize that pollutants in aqueous solution more easily carry out electrophilic attacks on the optimized matrix.

Table 2. The HSAB reactivity descriptors in the present study.

	GAP (eV)	I (eV)	A (eV)	χ (eV)	η (eV)	μ (eV)	S (eV ⁻¹)	ω (eV)
BN55	5.907	7.879	1.972	4.926	2.954	−4.926	0.169	4.107
BN55_CC1	5.773	7.773	2.000	4.887	2.887	−4.887	0.173	4.136
chl	8.170	9.140	0.970	5.055	4.085	−5.055	0.122	3.128
fen	8.235	9.343	1.108	5.226	4.118	−5.226	0.121	3.316
BN55_chl	5.892	7.868	1.976	4.922	2.946	−4.922	0.170	4.112
BN55_fen	5.864	7.843	1.979	4.911	2.932	−4.911	0.171	4.113
BN55_CC1_chl	5.712	7.713	2.001	4.857	2.856	−4.857	0.175	4.130
BN55_CC1_fen	5.721	7.804	2.083	4.944	2.861	−4.944	0.175	4.272
BN55_s	5.970	7.807	1.837	4.822	2.985	−4.822	0.168	3.895
BN55_CC1_s	5.888	7.759	1.871	4.815	2.944	−4.815	0.170	3.938
chl_s	8.230	9.370	1.140	5.255	4.115	−5.255	0.122	3.355
fen_s	8.143	9.486	1.343	5.415	4.072	−5.415	0.123	3.600
BN55_chl_s	5.941	7.753	1.812	4.783	2.971	−4.783	0.168	3.850
BN55_fen_s	5.937	7.749	1.812	4.781	2.969	−4.781	0.168	3.849
BN55_CC1_chl_s	5.803	7.632	1.829	4.731	2.902	−4.731	0.172	3.856
BN55_CC1_fen_s	5.798	7.657	1.859	4.758	2.899	−4.758	0.172	3.905
4pep_s	9.845	9.685	−0.160	4.763	4.923	−4.763	0.102	2.304
BN55_4pep_s	5.968	7.763	1.795	4.779	2.984	−4.779	0.168	3.827
BN55_CC1_4pep_s	5.913	7.729	1.816	4.773	2.957	−4.773	0.169	3.852
BN55_4pep_chl_s	5.932	7.683	1.751	4.717	2.966	−4.717	0.169	3.751
BN55_4pep_fen_s	5.969	7.779	1.810	4.795	2.985	−4.795	0.168	3.851
BN55_CC1_4pep_chl_s	5.729	7.526	1.797	4.662	2.865	−4.662	0.175	3.793
BN55_CC1_4pep_fen_s	5.890	7.707	1.817	4.762	2.945	−4.762	0.170	3.850

The chemical hardness of chlorpyrifos increases in water, while the reduction of fenitrothion is from 4.118 to 4.072. A change in polar properties can explain why the adsorption energy between chlorpyrifos and BN55-CC1-4pep is so small. The conclusion is that “soft” particles and “soft” particles or “hard” particles and “hard” particles form a strong bond, since C-doped promotes a decrease in the amount of change in chemical hardness, fenitrothion is more suitable for adsorption by BN55-CC1_s than chlorpyrifos, followed by BN55-CC1-4pep_s. Four nanomaterials show the enhancement of GAP, which has a positive relationship with chemical hardness. Thus, they could be more stable, especially in solution. In Table 2, the compound with the highest stability is the tetrapeptide. Both GAP and chemical hardness are at the maximum, indicating that it is hard to excite electrons during transition, so the molecular stability is extremely high. When BN55-4pep_s and BN55-CC1-4pep_s are combined with pollutants the GAP and chemical hardness values of fenitrothion/BN55-4pep and fenitrothion/BN55-CC1-4pep are greater than those of chlorpyrifos/BN55-4pep and chlorpyrifos/BN55-CC1-4pep, respectively, directly telling us that the former complexes are more stable.

The GAP of BN55_s is the largest among all nanoadsorbents. In fact, the addition of tetrapeptides and C-doping is conducive to the reduction of GAP, which will result in an increase in conductivity. The bandgap decreases gradually with the increase in C-doping with low charge transfer resistance [5]. In terms of electrical conductivity, the effect of C-doping is indeed more significant than that of tetrapeptide. The bonding states and antibonding states in h-BN are much stronger than those of graphene. When carbon

replaces boron atoms and nitrogen atoms, respectively, it forms extra electrons and electron holes and improves conductivity.

When a compound is added to change the energy band, the amount of change is greater, and there are more opportunities for material to be the sensor. Simultaneously, to prevent sensors from being destroyed, BN55-4pep and BN55-CC1-4pep avoid that problem due to their high adsorption energy in solution, according to Table 1. When a carbon is substituted in BNNT, the calculated band structures show that the defect electronic levels inside the band gap are sensitive to the presence of the adsorbed molecules [43]. BN55-CC1-4pep_s has the largest GAP change after adsorption of chlorpyrifos, which is as high as 0.184 eV. The GAP in BN55-CC1-4pep_s is 5.913 eV, indicating high conductivity. Therefore, the molecular recognition of chlorpyrifos is the best, although the adsorption energy is the lowest. The highest conductive, BN55-CC1_s, can detect fenitrothion via a GAP change of about 0.09 eV. The values of GAP change mentioned above are all the more obvious than the 0.05~0.06 eV from gaseous C-doped BNNT for both pesticides, indicating that they attribute their extraordinary results to aqueous sensors. BN55-CC1_s has excellent application of both removal and detection of fenitrothion among the four adsorbent materials.

4. Conclusions

The C-doping method contributes the most towards reducing the bandgap, and tetrapeptides can form hydrogen bonds with organophosphorus pesticides to strengthen non-covalent interactions. Compared with a gaseous environment, adsorption is improved in the aqueous phase. On the other hand, decorated boron nitride nanotubes as aqueous sensors are advantageous for organophosphorus pesticides in the solution due to the change in electronic structures, making themselves a stronger electron donor. BN55-CC1-4pep_s shows exceptional performance when detecting chlorpyrifos, which is shown that an AChE biosensor and organophosphorus pesticides are highly compatible in the previous reference. As far as fenitrothion is concerned, BN55-CC1_s exhibits high sensitivity and high stability. Not only is it suitable as a sensor, but it is also good at purification of the environment for fenitrothion, indicating that the biosensor faces selectivity toward organophosphorus pesticides. This is worth studying next time.

Author Contributions: Conceptualization, C.-L.L. and C.M.C.; methodology, C.-L.L. and C.M.C.; software, C.-L.L.; validation, C.M.C.; formal analysis, C.-L.L. and C.M.C.; investigation, C.-L.L.; resources, C.M.C.; data curation, C.-L.L.; writing—original draft preparation, C.-L.L.; writing—review and editing, C.M.C.; visualization, C.-L.L. and C.M.C.; supervision, C.M.C.; project administration, C.M.C.; funding acquisition, C.M.C. All authors have read and agreed to the published version of the manuscript.

Funding: This research was funded by the National Science Council of Taiwan, Republic of China and grant number [MOST 111-2321-B-005-004].

Institutional Review Board Statement: Not applicable.

Informed Consent Statement: Not applicable.

Data Availability Statement: Not applicable.

Acknowledgments: The authors thank the National Science Council of Taiwan, Republic of China, for providing financial support. Computer time was provided by the National Center for High-Performance Computing.

Conflicts of Interest: The authors declare no conflict of interest.

References

1. Pan, H.; Lei, H.; He, X.; Xi, B.; Xu, Q. Spatial distribution of organochlorine and organophosphorus pesticides in soil-groundwater systems and their associated risks in the middle reaches of the Yangtze River Basin. *Environ. Geochem. Health* **2019**, *41*, 1833–1845. [[CrossRef](#)] [[PubMed](#)]
2. Blase, X.; Rubio, A.; Louie, S.G.; Cohen, M.L. Stability and Band Gap Constancy of Boron Nitride Nanotubes. *Europhys. Lett. EPL* **1994**, *28*, 335–340. [[CrossRef](#)]
3. dos Santos, J.R.; da Silva, E.L.; de Oliveira, O.V.; dos Santos, J.D. Theoretical study of sarin adsorption on (12,0) boron nitride nanotube doped with silicon atoms. *Chem. Phys. Lett.* **2020**, *738*, 136816. [[CrossRef](#)]
4. Farmanzadeh, D.; Rezaeinejad, H. DFT Study of Adsorption of Diazinon, Hinosan, Chlorpyrifos and Parathion Pesticides on the Surface of B36N36 Nanocage and Its Fe Doped Derivatives as New Adsorbents. *Acta Phys. Chim. Sin.* **2016**, *32*, 1191–1198. [[CrossRef](#)]
5. Zhao, T.; Shi, J.; Huo, M.; Wan, R. Electronic properties of C-doped boron nitride nanotubes studied by first-principles calculations. *Phys. E Low Dimens. Syst. Nanostruct.* **2014**, *64*, 123–128. [[CrossRef](#)]
6. Zhao, J.; Chen, Z. Carbon-Doped Boron Nitride Nanosheet: An Efficient Metal-Free Electrocatalyst for the Oxygen Reduction Reaction. *J. Phys. Chem. C* **2015**, *119*, 26348–26354. [[CrossRef](#)]
7. Zhao, J.-X.; Dai, B.-Q. DFT studies of electro-conductivity of carbon-doped boron nitride nanotube. *Mater. Chem. Phys.* **2004**, *88*, 244–249. [[CrossRef](#)]
8. Chegel, R. Effects of carbon doping on the electronic properties of boron nitride nanotubes: Tight binding calculation. *Phys. E Low-Dimens. Syst. Nanostruct.* **2016**, *84*, 223–234. [[CrossRef](#)]
9. Farmanzadeh, D.; Rezaeinejad, H. Adsorption of parathion and chlorpyrifos organophosphorus pesticides with the iron doped boron nitride nanotubes; A theoretical study. *Appl. Chem.* **2017**, *12*, 215–232. [[CrossRef](#)]
10. Baierle, R.J.; Piquini, P.; Schmidt, T.M.; Fazzio, A. Hydrogen Adsorption on Carbon-Doped Boron Nitride Nanotube. *J. Phys. Chem. B* **2006**, *110*, 21184–21188. [[CrossRef](#)]
11. Esrafil, M.D.; Saeidi, N. Carbon-doped boron nitride nanosheet as a promising catalyst for N₂O reduction by CO or SO₂ molecule: A comparative DFT study. *Appl. Surf. Sci.* **2018**, *444*, 584–589. [[CrossRef](#)]
12. Liu, Z.; Zhang, M.; Wang, H.; Cang, D.; Ji, X.; Liu, B.; Yang, W.; Li, D.; Liu, J. Defective Carbon-Doped Boron Nitride Nanosheets for Highly Efficient Electrocatalytic Conversion of N₂ to NH₃. *ACS Sustain. Chem. Eng.* **2020**, *8*, 5278–5286. [[CrossRef](#)]
13. Millard, C.B.; Kryger, G.; Ordentlich, A.; Greenblatt, H.M.; Harel, M.; Raves, M.L.; Segall, Y.; Barak, D.; Shafferman, A.; Silman, I.; et al. Crystal Structures of Aged Phosphorylated Acetylcholinesterase: Nerve Agent Reaction Products at the Atomic Level. *Biochemistry* **1999**, *38*, 7032–7039. [[CrossRef](#)] [[PubMed](#)]
14. Mascini, M.; Carlo, M.D.; Compagnone, D. Development OF Artificial Oligopeptides as Biomimetic Receptors for Carbamate and Organophosphate Pesticides Using a Computational Approach. In *Sensors and Microsystems*; Springer: Cham, Switzerland, 2005; pp. 44–49.
15. Mascini, M.; Sergi, M.; Monti, D.; Carlo, M.D.; Compagnone, D. Oligopeptides as Mimic of Acetylcholinesterase: From the Rational Design to the Application in Solid-Phase Extraction for Pesticides. *Anal. Chem.* **2008**, *80*, 9150–9156. [[CrossRef](#)]
16. Cui, H.-F.; Wu, W.-W.; Li, M.-M.; Song, X.; Lv, Y.; Zhang, T.-T. A highly stable acetylcholinesterase biosensor based on chitosan-TiO₂-graphene nanocomposites for detection of organophosphate pesticides. *Biosens. Bioelectron.* **2018**, *99*, 223–229. [[CrossRef](#)]
17. Baker, P.A.; Goltz, M.N.; Schrand, A.M.; Kim, D.-S. Organophosphate vapor detection on gold electrodes using peptide nanotubes. *Biosens. Bioelectron.* **2014**, *61*, 119–123. [[CrossRef](#)]
18. Periasamy, A.P.; Umasankar, Y.; Chen, S.-M. Nanomaterials-Acetylcholinesterase Enzyme Matrices for Organophosphorus Pesticides Electrochemical Sensors: A Review. *Sensors* **2009**, *9*, 4034–4055. [[CrossRef](#)]
19. Zhiani, R. Adsorption of various types of amino acids on the graphene and boron-nitride nano-sheet, a DFT-D3 study. *Appl. Surf. Sci.* **2017**, *409*, 35. [[CrossRef](#)]
20. Chen, D.; Liu, Z.; Fu, J.; Guo, Y.; Sun, X.; Yang, Q.; Wang, X. Electrochemical acetylcholinesterase biosensor based on multi-walled carbon nanotubes/dicyclohexyl phthalate modified screen-printed electrode for detection of chlorpyrifos. *J. Electroanal. Chem.* **2017**, *801*, 185–191. [[CrossRef](#)]
21. Amine, A.; Mohammadi, H.; Bourais, I.; Palleschi, G. Enzyme inhibition-based biosensors for food safety and environmental monitoring. *Biosens. Bioelectron.* **2006**, *21*, 1405–1423. [[CrossRef](#)]
22. Brljak, N.; Parab, A.D.; Rao, R.; Slocik, J.M.; Naik, R.R.; Knecht, M.R.; Walsh, T.R. Material composition and peptide sequence affects biomolecule affinity to and selectivity for h-boron nitride and graphene. *Chem. Commun.* **2020**, *56*, 8834–8837. [[CrossRef](#)]
23. Fang, D.; Chaudret, R.; Piquemal, J.-P.; Cisneros, G.A. Toward a Deeper Understanding of Enzyme Reactions Using the Coupled ELF/NCI Analysis: Application to DNA Repair Enzymes. *J. Chem. Theory Comput.* **2013**, *9*, 2156–2160. [[CrossRef](#)]
24. Andrés, J.; Berski, S.; Contreras-García, J.; González-Navarrete, P. Following the Molecular Mechanism for the NH₃ + LiH → LiNH₂ + H₂ Chemical Reaction: A Study Based on the Joint Use of the Quantum Theory of Atoms in Molecules (QTAIM) and Noncovalent Interaction (NCI) Index. *J. Phys. Chem. A* **2014**, *118*, 1663–1672. [[CrossRef](#)]
25. de Courcy, B.; Pedersen, L.G.; Parisel, O.; Gresh, N.; Silvi, B.; Pilmé, J.; Piquemal, J.P. Understanding Selectivity of Hard and Soft Metal Cations within Biological Systems Using the Subvalence Concept. 1. Application to Blood Coagulation: Direct Cation–Protein Electronic Effects versus Indirect Interactions through Water Networks. *J. Chem. Theory Comput.* **2010**, *6*, 1048–1063. [[CrossRef](#)]

26. Bergès, J.; Fourré, I.; Pilmé, J.; Kozelka, J. Quantum Chemical Topology Study of the Water-Platinum(II) Interaction. *Inorg. Chem.* **2013**, *52*, 1217–1227. [[CrossRef](#)]
27. Tantardini, C.; Benassi, E. Topology vs. thermodynamics in chemical reactions: The instability of PH₅. *Phys. Chem. Chem. Phys.* **2017**, *19*, 27779–27785. [[CrossRef](#)]
28. Lazarević-Pašti, T.; Aničijević, V.; Baljžović, M.; Aničijević, D.V.; Gutić, S.; Vasić, V.; Skorodumova, N.V.; Pašti, I.A. The impact of the structure of graphene-based materials on the removal of organophosphorus pesticides from water. *Environ. Sci. Nano* **2018**, *5*, 1482–1494. [[CrossRef](#)]
29. Mohammed, M.H. Electronic and thermoelectric properties of zigzag and armchair boron nitride nanotubes in the presence of C island. *Chin. J. Phys.* **2018**, *56*, 1622–1632. [[CrossRef](#)]
30. He, Z.; Zhou, J. Probing carbon nanotube–amino acid interactions in aqueous solution with molecular dynamics simulations. *Carbon* **2014**, *78*, 500–509. [[CrossRef](#)]
31. Walsh, T.R.; Knecht, M.R. Biomolecular Material Recognition in Two Dimensions: Peptide Binding to Graphene, h-BN, and MoS₂ Nanosheets as Unique Bioconjugates. *Bioconjugate Chem.* **2019**, *30*, 2727–2750. [[CrossRef](#)] [[PubMed](#)]
32. Stewart, J.J. Optimization of parameters for semiempirical methods VI: More modifications to the NDDO approximations and re-optimization of parameters. *J. Mol. Modeling* **2013**, *19*, 1–32. [[CrossRef](#)]
33. Johnson, E.R.; Keinan, S.; Mori-Sánchez, P.; Contreras-García, J.; Cohen, A.J.; Yang, W. Revealing Noncovalent Interactions. *J. Am. Chem. Soc.* **2010**, *132*, 6498–6506. [[CrossRef](#)] [[PubMed](#)]
34. Contreras-García, J.; Johnson, E.R.; Keinan, S.; Chaudret, R.; Piquemal, J.-P.; Beratan, D.N.; Yang, W. NCIPLOT: A Program for Plotting Noncovalent Interaction Regions. *J. Chem. Theory Comput.* **2011**, *7*, 625–632. [[CrossRef](#)] [[PubMed](#)]
35. Braga, L.S.; Leal, D.H.; Kuca, K.; Ramalho, T.C. Perspectives on the Role of the Frontier Effective-for-Reaction Molecular Orbital (FERMO) in the Study of Chemical Reactivity: An Updated Review. *Curr. Org. Chem.* **2020**, *24*, 314–331. [[CrossRef](#)]
36. Zhuo, L.G.; Liao, W.; Yu, Z.X. A frontier molecular orbital theory approach to understanding the Mayr equation and to quantifying nucleophilicity and electrophilicity by using HOMO and LUMO energies. *Asian J. Org. Chem.* **2012**, *1*, 336–345. [[CrossRef](#)]
37. Yang, Z.; Wang, Z.; Tian, X.; Xiu, P.; Zhou, R. Amino acid analogues bind to carbon nanotube via π - π interactions: Comparison of molecular mechanical and quantum mechanical calculations. *J. Chem. Phys.* **2012**, *136*, 01B607. [[CrossRef](#)]
38. Gao, Z.; Zhi, C.; Bando, Y.; Golberg, D.; Serizawa, T. Isolation of Individual Boron Nitride Nanotubes via Peptide Wrapping. *J. Am. Chem. Soc.* **2010**, *132*, 4976–4977. [[CrossRef](#)]
39. Rimola, A. Intrinsic Ladders of Affinity for Amino-Acid-Analogues on Boron Nitride Nanomaterials: A B3LYP-D2* Periodic Study. *J. Phys. Chem. C* **2015**, *119*, 17707–17717. [[CrossRef](#)]
40. Santos, G.P.d.; Silva, B.F.d.; Garrido, S.S.; Mascini, M.; Yamanaka, H. Design, synthesis and characterization of a hexapeptide bio-inspired by acetylcholinesterase and its interaction with pesticide dichlorvos. *Analyst* **2014**, *139*, 273–279. [[CrossRef](#)]
41. Bo, X.; Zhou, M.; Guo, L. Electrochemical sensors and biosensors based on less aggregated graphene. *Biosens. Bioelectron.* **2017**, *89*, 167–186. [[CrossRef](#)]
42. Villanueva-Mejia, F.; Navarro-Santos, P.; Rodríguez-Kessler, P.L.; Herrera-Bucio, R.; Rivera, J.L. Reactivity of Atomically Functionalized C-Doped Boron Nitride Nanoribbons and Their Interaction with Organosulfur Compounds. *Nanomaterials* **2019**, *9*, 452. [[CrossRef](#)]
43. Baierle, R.J.; Schmidt, T.M.; Fazzio, A. Adsorption of CO and NO molecules on carbon doped boron nitride nanotubes. *Solid State Commun.* **2007**, *142*, 49–53. [[CrossRef](#)]